

# Heterogeneity within Order in Crystals of a Porous Metal–Organic Framework

Kyung Min Choi,<sup>†</sup> Hyung Joon Jeon,<sup>†</sup> Jeung Ku Kang,<sup>\*,†,‡</sup> and Omar M. Yaghi<sup>\*,‡,§</sup>

<sup>†</sup>Department of Materials Science and Engineering and <sup>‡</sup>NanoCentury KAIST Institute and Graduate School of EEWs (WCU), Korea Advanced Institute of Science and Technology (KAIST), 373-1, Guseong Dong, Yuseong Gu, Daejeon 305-701, Republic of Korea

<sup>§</sup>Center for Reticular Chemistry, Center for Global Mentoring, UCLA-DOE Institute for Genomics and Proteomics, and Department of Chemistry and Biochemistry, University of California - Los Angeles, 607 Charles E. Young Drive, East, Los Angeles, California 90095, United States

**S** Supporting Information

**ABSTRACT:** Generally, crystals of synthetic porous materials such as metal–organic frameworks (MOFs) are commonly made up from one kind of repeating pore structure which predominates the whole material. Surprisingly, little is known about how to introduce heterogeneously arranged pores within a crystal of homogeneous pores without losing the crystalline nature of the material. Here, we outline a strategy for producing crystals of MOF-5 in which a system of meso- and macropores either permeates the whole crystal to make sponge-like crystals or is entirely enclosed by a thick crystalline microporous MOF-5 sheath to make pomegranate-like crystals. These new forms of crystals represent a new class of materials in which micro-, meso-, and macroporosity are juxtaposed and are directly linked unique arrangements known to be useful in natural systems but heretofore unknown in synthetic crystals.

Crystals of synthetic compounds are typically composed of one kind of repeating structure, and thus their functionality is limited to a great extent by their lack of complexity. Strategies for making crystals of materials that encompass structural heterogeneity without losing their overall crystalline order are largely absent. This is because the synthetic methods used to produce crystals rely on optimization of reaction conditions to give crystallized products with homogeneous structures (Scheme 1a), and when this is not possible, amorphous structures are produced. We believe that vast opportunities exist for developing synthetic methods which combine the optimization for crystal formation while being amenable to the introduction of heterogeneous structures within a crystal as illustrated in Scheme 1b and c. On a fundamental level, we envision that these unique constructs, in which variously shaped compartments are directly linked, may be designed to have a range of scales and functionality allowing them to operate independently. This concept is widely used in natural systems but remains a challenge to introduce into synthetic crystals. In this report, we show how crystals of metal–organic framework-5 (MOF-5, Scheme 1a) can be prepared to have a heterogeneous arrangement of macro- and mesopores, which permeate a crystalline body to give a structure akin to a sponge (spng-MOF-5, Scheme 1b). We further show how this arrangement can be entirely enclosed by a thick crystalline microporous MOF-5 to make an overall

structure similar to that of a pomegranate (pmg-MOF-5, Scheme 1c). Remarkably, the entire bodies of spng-MOF-5 and pmg-MOF-5 are crystalline, have precisely the MOF-5 composition,  $Zn_4O(O_2CC_6H_4CO_2)_3$ , and show permanent porosity and robust architectures. The unusual structure of pmg-MOF-5 is found to have carbon dioxide adsorption properties unobserved for the original MOF-5.

Previous work has focused on the assembly of organic<sup>1</sup> and inorganic constituents<sup>2</sup> into core–shell structures; however, the core and shell either have a different composition or are non-porous. Although the well-known mesoporous silicates have ordered pores, they tend to have amorphous walls,<sup>3</sup> and porous carbon is entirely amorphous.<sup>4</sup> To date, there are no reports of porous crystals where the pores either are made from crystalline walls (Scheme 1b) or are completely enclosed by a microporous crystalline body (Scheme 1c). The present report describes a general method for producing such materials and uses as an exemplar the well-known MOF-5 structure. Our strategy for achieving spng- and pmg-MOF-5 is to assemble the MOF structure in the presence of carefully controlled amounts of 4-(dodecyloxy)benzoic acid (DBA, Scheme 1d). DBA serves the dual purpose of having a carboxyl functionality for binding to the metal, which is required for MOF formation, and an alkyl chain for space filling. Three lines of experimentation were carried out which, as we discuss below, reveal the decisive role of DBA: (1) in the absence of DBA, the usual MOF-5 crystals are produced as in Scheme 1a and e, (2) in the presence of amounts of DBA equimolar to that of the organic linker, MOF-5 crystals are produced but with macroscopic pores being visible at the crystal surface to give an overall spongy structure, spng-MOF-5, as illustrated in Scheme 1b and f, and (3) with the 30 mol % of DBA to the organic linker, MOF-5 crystals are produced, but these have the pomegranate-type of structure with a spongy core and solid outer shell, pmg-MOF-5 (Scheme 1c and g).

Crystals of MOF-5 and spng- and pmg-MOF-5 were prepared by adding  $Zn(NO_3)_2 \cdot 4H_2O$  to a *N,N*-diethylformamide solution mixture of terephthalic acid, and in the case of spng- and pmg-MOF-5, DBA was added in 30 and 50 mol % quantities to terephthalic acid, under conditions similar to those previously used in the synthesis of MOF-5<sup>5</sup> (Scheme 1e, f, and g). All the compounds were characterized by powder X-ray diffraction

Received: May 25, 2011

Published: July 12, 2011

Scheme 1

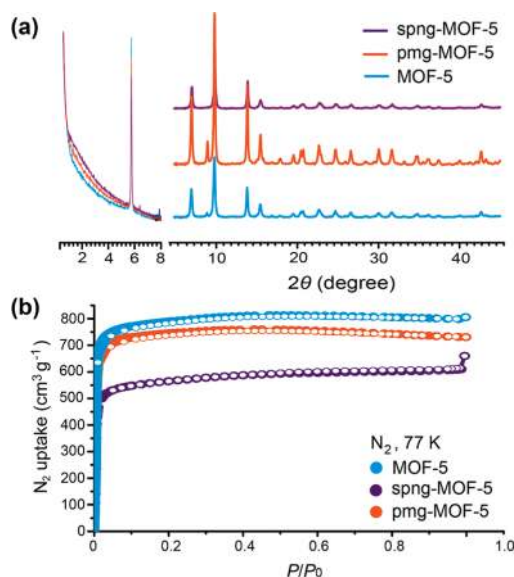
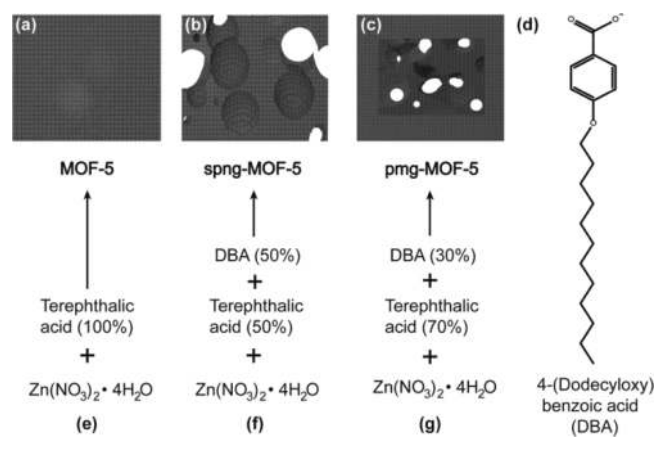


**Figure 1.** Typical analysis performed on MOF-5, spng-MOF-5, and pmg-MOF-5. (a) X-ray data of crystalline powder of MOF-5, spng-MOF-5, and pmg-MOF-5, (b)  $\text{N}_2$  adsorption isotherm at 77 K with adsorption (●) and desorption points (○).  $P/P_0$ , relative pressure.

(PXRD), transmission electron microscopy (TEM), nitrogen gas adsorption measurements, and scanning electron microscopy (SEM) to study their crystallinity, permanent porosity, and the formation of amorphous meso- and macropores, respectively. The pore structures of these compounds were also studied by dye inclusion into the pores and confocal microscopy as well as SEM measurements.

High crystallinity of MOF-5 and spng- and pmg-MOF-5 materials was evident from the sharp diffraction lines of their PXRD patterns (Figure 1a), and preservation of the MOF-5 structure arrangement in spng- and pmg-MOF-5 is also observed by coincidence of diffraction lines of all three PXRD patterns. Dark-field diffraction images from TEM analysis performed on the interior portion of the pmg-MOF-5 crystals showed strong diffractions; further supporting their uniformity (Figure S1 in the Supporting Information [SI]).<sup>6</sup> The presence of meso- and macropores in bulk spng- and pmg-MOF-5 samples was confirmed by the

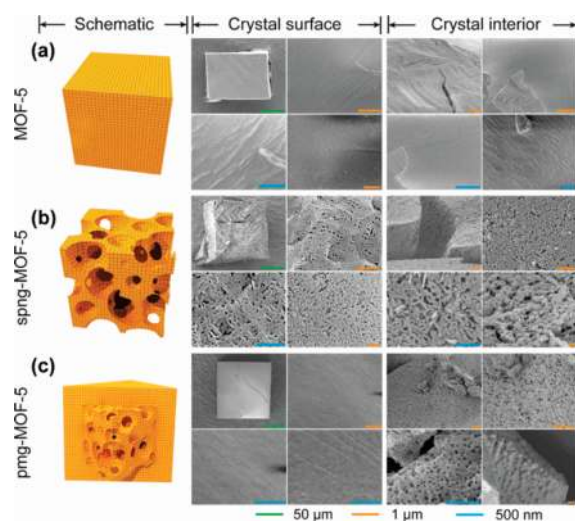


**Figure 2.** Pore structures of MOF-5, spng-MOF-5, and pmg-MOF-5 revealed by SEM observation of their crystal surface and interior (scale bars, green 50  $\mu\text{m}$ , red 1  $\mu\text{m}$ , blue 500 nm).

small-angle scattering using synchrotron X-ray (using synchrotron radiation at BL02B2 at SPring-8, Japan) (Figure 1a). The permanent porosity of evacuated spng- and pmg-MOF-5 was confirmed by measurement of the nitrogen gas-adsorption isotherm, which exhibited a type I behavior similar to that observed in MOF-5 (Figure 1b). The Langmuir surface areas of spng- and pmg-MOF-5 were calculated to be  $2560 \text{ m}^2 \text{ g}^{-1}$  and  $3230 \text{ m}^2 \text{ g}^{-1}$ , respectively. These values are within the range of what is considered to be ultrahigh surface areas for MOFs (the surface area of MOF-5 in this study is  $3410 \text{ m}^2 \text{ g}^{-1}$ ) and exceed those reported for porous zeolites, mesoporous silicas, and porous carbon.<sup>3,4,7</sup>

The unusual nature of spng- and pmg-MOF-5 crystals was uncovered by examining the crystal surface and interior using SEM (Figure 2). As expected, the as-synthesized MOF-5 crystals show a very smooth surface and interior (Figure 2a). However, meso- and macropores in the range of 10 nm – 100 nm were observed for both the surface and the interior of spng-MOF-5 (Figure 2b) that, when taken along with the PXRD evidence discussed above, supports the proposed crystalline spongy morphology. In the case of pmg-MOF-5, the surface was found to be strikingly smooth, as was the case for MOF-5, and the interior was found to be riddled with meso- and macropores in close resemblance and scale to those observed for spng-MOF-5 (Figure 2c). This evidence coupled to the sharp lines observed in the PXRD pattern of pmg-MOF-5, lends support to the proposed pomegranate-like morphology where a thick crystalline microporous MOF-5 exterior encloses a crystalline spongelike interior, and together encompass heterogeneous pores. This distinct morphology of pmg-MOF-5 was substantiated again with the type-I behavior in nitrogen gas-adsorption isotherm; the condensed-phase nitrogen fluid in a thick microporous exterior at pressure higher than that for micropore condensation ( $>0.05 P/P_0$  at 77 K with  $\text{N}_2$ ) blocks the penetration of nitrogen gas molecules from outside to the meso- and macroporous interior, thus making sorption behavior the same as that of MOF-5.<sup>8</sup>

Further evidence supporting the unique morphologies of spng- and pmg-MOF-5 was obtained by adding to the initial MOF reaction mixture a small amount ( $<10^{-4}$  mol %) of the molecular dye, rhodamine, and examining the extent of dye

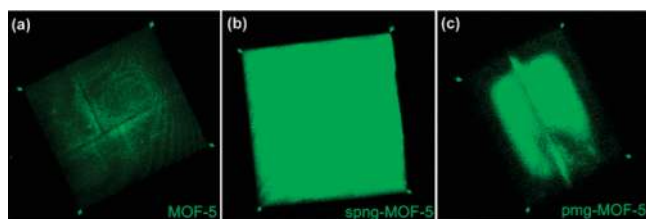


**Figure 3.** Confocal microscopy images of MOF-5, spng-MOF-5, and pmg-MOF-5 crystals, all including molecular dye, supporting their morphologies.

incorporation into the MOF crystal. Since rhodamine is approximately 1 nm in diameter, similar in size to that of the micropores of MOF-5 (aperture and pore size of 0.8 and 1.2 nm) but much smaller than the meso- and macropores in spng- and pmg-MOF-5, thus it was anticipated that it would be preferably incorporated in the meso- and macropores rather than the micropores. Indeed, examination of the crystals, obtained from the dye containing reactions for all three MOFs, by confocal microscopy reveals an intense luminescence in the meso- and macroporous region of the crystals, which is attributable to the larger concentration of dye in those regions (Figure 3). It is clear from the forgoing observations that the unusual nature of spng-MOF-5 and more specially that of pmg-MOF-5 crystals are directly related to the availability of DBA which attaches to the growing crystal using carboxyl functionality and hampers the local crystal growth to make meso- and macropores using the alkyl chain in the nucleation and crystal growth steps. In the case of spng-MOF-5 where large amounts of DBA are available, the meso- and macroporous system permeates from the center to the surface of the crystals. With lesser amounts of DBA present in the reaction, the crystals are 'starved' of DBA at the midpoint during crystal growth, leading to a meso- and macroporous interior and a microporous exterior. The forgoing discussion clarifies that there is direct correspondence between the amount of DBA used and the nature of the product. Also, the solution  $^1\text{H}$  nuclear magnetic resonance (NMR) of digested spng- and pmg-MOF-5 reveals that DBA is removed from the crystals by the solvent exchange during the activation processes and no DBA remains in the activated crystals (Figure S11 in the SI).<sup>6</sup> This synthetic strategy is quite reproducible in that the synthesis of these unusual crystals has been carried out well over two dozen times, giving identical results as presented above. It should be noted that this strategy also yields homogeneous bulk materials: several different crystals randomly selected from the different batches show identical results for each of the three MOFs.<sup>6</sup>

We studied the  $\text{CO}_2$  adsorptive properties of these MOFs and found that pmg-MOF-5 takes up much more  $\text{CO}_2$  ( $2.0 \text{ g g}^{-1}$  at 195 K and 760 Torr) than MOF-5 ( $\text{CO}_2$ :  $1.5 \text{ g g}^{-1}$  at 195 K and 760 Torr)<sup>9</sup> (Figure 4a). This is despite the fact that pmg-MOF-5 ( $3230 \text{ m}^2 \text{ g}^{-1}$ ) has less surface area than MOF-5 ( $3410 \text{ m}^2 \text{ g}^{-1}$ ), an observation which points to the unusual nature of the internal surface of the meso- and macropores and the likely presence of a higher concentration of defects relative to MOF-5. The uptake behavior of pmg-MOF-5 is quite distinct from that of MOF-5. The initial uptake up to 160 Torr is linear as in MOF-5, but the pressure of the inflection shifts toward to 220 Torr, and uptake continuously increases from that point up to 760 Torr (Figure 4a). This behavior is consistent with having carbon dioxide uptake into the microporous region of pmg-MOF-5

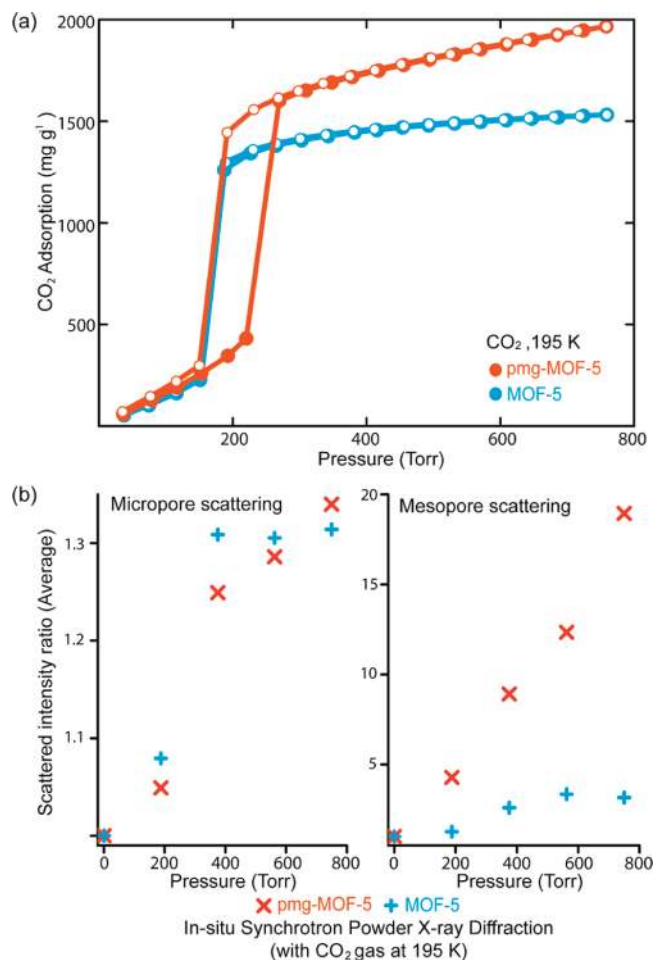


**Figure 4.**  $\text{CO}_2$  adsorptive properties for pmg-MOF-5 and MOF-5. (a)  $\text{CO}_2$  uptake at 195 K for pmg-MOF-5 (red) and MOF-5 (blue), adsorption (●) and desorption (○), respectively. Connecting lines are guides for the eyes. (b) In situ synchrotron powder X-ray diffraction as a function of gas pressure for pmg-MOF-5 (red) and MOF-5 (blue). The standard value for scattered intensity ratio is the peak intensity at 0 Torr.

crystals first; then as the pressure is increased, it fills through the interface of the meso- and macropore region. Whereas the desorption behavior of pmg-MOF-5 is similar to that of MOF-5, all gas molecules in the crystals flow out through microporous outer shell, and thus hysteresis. This additional  $\text{CO}_2$  adsorption into the meso- and macropores of pmg-MOF-5 was confirmed by the in situ synchrotron powder X-ray diffraction of gas adsorption<sup>10</sup> (using synchrotron radiation at BL02B2 at SPring-8, Japan) (Figure 4b). Scattered X-rays from adsorbed  $\text{CO}_2$  in pmg-MOF-5 increase peak intensity in both micropore and mesopore regions, while MOF-5 has intensity only in the micropore region;<sup>6</sup> a result which indicates an additional  $\text{CO}_2$  adsorption through the interface of the mesopores in pmg-MOF-5.

The porous MOF crystals reported here represent a new class of porous crystals where the micro-, meso-, and macroporosity are juxtaposed and/or completely enclosed by a microporous crystalline body. The strategy of using controlled amounts of DBA to punctuate the progression pores should be effective at generating a large number of unique crystalline constructions where heterogeneity is contained within order without losing either crystallinity or porosity.

## ■ ASSOCIATED CONTENT

**S Supporting Information.** Synthesis and characterization of spng-MOF-5 and pmg-MOF-5. This material is available free of charge via the Internet at <http://pubs.acs.org>.

## ■ AUTHOR INFORMATION

### Corresponding Author

jeungku@kaist.ac.kr, yaghi@chem.ucla.edu

## ■ ACKNOWLEDGMENT

We acknowledge the World Class University Program for the financial support (R-31-2008-000-10055-0). This study was also supported by JASRI/SPRING-8. We thank Prof. Osamu Terasaki and Dr. Keiichi Miyasaka (KAIST) for assistance and helpful discussion with SEM, and acknowledge the invaluable discussion of Drs. Hiroyasu Furukawa (Yaghi research group) and Yoshiki Kubota (Osaka Prefecture University).

## ■ REFERENCES

- (1) (a) Ishizu, K. *Prog. Polym. Sci.* **1998**, *23*, 1383. (b) Rieter, W. J.; Taylor, K. M. L.; Lin, W. *J. Am. Chem. Soc.* **2008**, *129*, 9852. (c) Koh, K.; Wong-Foy, A. G.; Matzger, A. J. *Chem. Commun.* **2009**, *41*, 6162.
- (2) (a) Joo, S. H.; Park, J. Y.; Tsung, C. K.; Yamada, Y.; Yang, P.; Somorjai, G. A. *Nat. Mater.* **2009**, *8*, 126. (b) Xu, Z.; Hou, Y.; Sun, S. *J. Am. Chem. Soc.* **2007**, *129*, 8698. (c) Choi, K. M.; Augustine, S.; Choi, J. H.; Lee, J. H.; Shin, W. H.; Yang, S. H.; Lee, J. Y.; Kang, J. K. *Angew. Chem., Int. Ed.* **2008**, *47*, 9904.
- (3) (a) Han, Y.; Zhang, D.; Chung, L. L.; Sun, J.; Zhao, L.; Zou, X.; Ying, J. Y. *Nature Chem.* **2009**, *1*, 123. (b) Wan, Y.; Zhao, D. Y. *Chem. Rev.* **2007**, *107*, 2821. (c) Inagaki, S.; Guan, S.; Ohsuna, T.; Terasaki, O. *Nature* **2002**, *416*, 304.
- (4) (a) Liang, C.; Li, Z.; Dai, S. *Angew. Chem., Int. Ed.* **2008**, *47*, 3696. (b) Su, D. S.; Chen, X.; Weinberg, G.; Kellin-Hofmann, A.; Timpe, O.; Hamid, S. B.; Schlögl, R. *Angew. Chem., Int. Ed.* **2005**, *44*, 5488. (c) Yang, R. T. *Adsorbents: Fundamentals and Applications*; Wiley-Interscience: New York, 2003.
- (5) (a) Li, H.; Eddaoudi, M.; O'Keeffe, M.; Yaghi, O. M. *Nature* **1999**, *402*, 276. (b) Eddaoudi, M.; Kim, J.; Rosi, N.; Vodak, D.; Wachter, J.; O'Keeffe, M.; Yaghi, O. M. *Science* **2002**, *295*, 469.
- (6) See the SI.
- (7) Baerlocher, C.; Meier, W. M.; Olson, D. H. *Atlas of Zeolite Framework Types*, 5th ed.; Elsevier: Amsterdam, 2001.
- (8) For spng-MOF-5, a large amount of DBAs results in large-sized macropores (>80 nm) for most of pores except micropores (Figure 2). However, macropores are not observed by conventional isotherm measurements, because the pore filling would occur at pressures too close to the vapor pressure.
- (9) Walton, K. S.; Millward, A. R.; Dubbeldam, D.; Frost, H.; Low, L. L.; Yaghi, O. M.; Snurr, R. Q. *J. Am. Chem. Soc.* **2008**, *130*, 406.
- (10) (a) Kubota, Y.; Takata, M.; Kobayashi, T. C.; Kitagawa, S. *Coord. Chem. Rev.* **2007**, *251*, 2510. (b) Muroyama, N.; Yoshimura, A.; Kubota, Y.; Miyasaka, K.; Ohsuna, T.; Ryoo, R.; Ravikovitch, P.; Neimark, A. V.; Takata, M.; Terasaki, O. *J. Phys. Chem. C* **2008**, *112*, 10803.